EFFICIENT SIMULATION OF PARTICLE–LADEN TURBULENT FLOWS WITH HIGH MASS LOADINGS USING LES

M. Breuer and M. Alletto
Department of Fluid Mechanics
Helmut–Schmidt–University Hamburg
Holstenhofweg 85, D–22043 Hamburg, Germany
breuer/alletto@hsu-hh.de

ABSTRACT

The paper is concerned with the simulation of particle–laden two–phase flows based on the Euler–Lagrange approach. The methodology developed is driven by two compulsory requirements: (i) the necessity to tackle complex turbulent flows by eddy–resolving schemes such as large–eddy simulation; (ii) the demand to predict dispersed multiphase flows at high mass loadings. First, a highly efficient particle tracking algorithm was developed working on curvilinear, block–structured grids. Second, to allow the prediction of dense two–phase flows, the fluid-particle interaction (two–way coupling) as well as particle-particle collisions (four–way coupling) had to be taken into account. For the latter instead of a stochastic collision model, in the present study a deterministic collision model is considered. Nevertheless, the computational burden is minor owing to the concept of virtual cells, where only adjacent particles are taken into account in the search for potential collision partners. The methodology is applied to different test cases (plane channel flow, combustion chamber flow). The computational results are compared with experimental measurements and an encouraging agreement is found.

INTRODUCTION

Turbulent dispersed multiphase flows play an important role in many technical as well as medical applications such as cyclones, filters or inhalators. Up to now, most of the numerical investigations were based on the Reynolds–Averaged Navier–Stokes equations (RANS) combined with statistical turbulence models. Since in the majority of flows considered complex phenomena such as curved streamlines, secondary flow regions and transition are involved, the continuous phase is not predicted reliably by RANS. Consequently, the prediction of particle motion and deposition using a Lagrangian random–walk eddy–interaction model or similar methods to track the particles in the flow field was often found to be not accurate enough.

Therefore, during the last years huge effort was directed towards a methodology which is much more appropriate for the simulation of the continuous phase of turbulent flows including complex flow phenomena, i.e., the large–eddy simulation (LES) technique. However, the computational resources required for LES are very large. Predicting the particulate phase by a Lagrangian particle tracking further increases the computational requirements. Thus a highly efficient tracking algorithm is a must. This is the first issue addressed in this paper. Furthermore, since dense two–phase flows are of particular interest, physical effects such as the fluid–particle interaction (two–way coupling) as well as particle–particle collisions (four–way coupling) have to be taken into account. Especially the latter phenomenon may lead to a enormous computational burden if not tackled reasonably. That is the second issue considered. To the best of our knowledge, the work presents the first four–way coupled simulation in complex geometries using LES and a Lagrangian particle tracking with deterministic collision detection. The procedure is validated based on particle–laden channel flow and presently also applied to the experimental data of the particle–laden flow in a model combustion chamber (Boree et al., 2001).

COMPUTATIONAL METHODOLOGY

The method relies on the Euler–Lagrange approach where the continuous phase is simulated in the Eulerian frame of reference using LES, whereas for the particulate phase a huge number of individual particles is tracked throughout the computational domain in a Lagrangian frame of reference.

Continuous Phase

For the prediction of the fluid phase based on LES the filtered Navier–Stokes equations are taken into account. They are discretized by a standard 3–D finite–volume method for arbitrary non–orthogonal and block–structured grids within the LES code LESOCC (Breuer, 1998; 2002). The spatial discretization of all fluxes is based on central differences of second–order accuracy. A low–storage multi–stage Runge–Kutta method (second–order accurate) is applied for time–marching. In order to ensure the coupling of pressure and velocity fields on non–staggered grids, the momentum interpolation technique is used. For modeling the non–resolvable subgrid scales, two different models are applied, namely the well–known Smagorinsky model (1963) with Van Driest damping near solid walls ($C_s = 0.065$) and the dynamic approach with a Smagorinsky base model proposed by Germano et al. (1991)

and modified by Lilly (1992). The code is highly vectorized and additionally parallelized by domain decomposition using MPI.

Coupling of Continuous and Dispersed Phase

In order to track particles through the continuous flow field as described in the next section, the (filtered) fluid velocity at the particle position is required. Presently, it is interpolated using a Taylor series expansion around the cell center next to the particle (Marchioli et al., 2007). This interpolation scheme was shown to possess a weaker filtering effect on the fluid velocity than a trilinear interpolation used before (Breuer et al., 2006, 2007) leading to better results for particles with small relaxation times.

If for tiny particles their relaxation time is of the same order as the smallest fluid time scales, the unresolved scales become important for the particle motion. To consider the effect of the subgrid scales a simple stochastic model by Pozorski et al. (2009) is applied. It requires the estimation of the subgrid–scale kinetic energy carried out with the help of the scale similarity approach of Bardina et al. (1980).

Restricting the interaction of fluid and particles to these effects is called *one–way coupling* and only valid for volume fractions below about 10^{-6} (Sommerfeld, 2000). Above this limit the influence of the particles on the fluid motion has to be taken into account, leading to a *two–way coupled* simulation. For that purpose the particle-source-in-cell (PISC) method by Crowe et al. (1977) is used accounting for the exchange of momentum. This leads to a modified filtered Navier–Stokes equation with an additional source term representing the forces exerted by the particles onto the fluid. A smooth source term distribution is achieved by trilinear distributing the contribution of the particle to the 8 cell centers surrounding the particle. When the volume fraction becomes larger than 10^{-3} (Sommerfeld, 2000) the regime of dilute dispersed two–phase flows is left. Then particle–particle collisions play an important role and have to be taken into account which is denoted *four–way coupling* (see next section).

Dispersed Phase

The dispersed phase is computed based on Newton's second law taking only drag, lift, gravity and buoyancy into account. Owing to high density ratios ($\rho_p/\rho_f \gg 1$) considered, all other contributions can be neglected. The particles are assumed to be rigid and spherical. No Brownian motion of the particles is taken into account since the particle sizes are large enough ($d_p \gtrsim 1\mu m$) to neglect its effect. The drag force on the particle is based on Stokes flow around a sphere improved by a correction factor defined by Schiller and Naumann (1933) in order to extent the validity of the relation for the drag coefficient towards higher particle Reynolds numbers ($0 < Re_p \leq 800$). The lift force acting on particles in shear flows is modeled by a formulation provided by McLaughlin (1991) for unbounded flows. If the particle lags behind the fluid, the resulting lift force experienced by the particle drives it in the direction of positive velocity gradient. The presence of a wall further affects the lift force, which can be accounted for by an extended model. Since the implementation of this model in a general–purpose curvilinear code is not trivial, it was presently not considered. However, in principle also this

effect can be incorporated if required. This might be done within further studies.

The numerical procedure is as follows. The ordinary differential equation for the particle velocity is integrated by a fourth–order Runge–Kutta scheme in physical space. For that purpose the local instantaneous flow velocities at the position of the particle is interpolated as mentioned above. In order to enable efficient tracking of millions of particles on a block–structured curvilinear grid, the second integration required to get the new location of the particle is done in the *computational space* (ξ, η, ζ; c–space) rather than in the physical space (x, y, z; p–space), see Breuer et al. (2006; 2007). In c–space schemes the particle traces are integrated in a coordinate system, in which the curvilinear physical space grid is orthonormal. Point location within the c–space grid is as trivial as for a Cartesian grid, since there is an explicit relationship between the c–space coordinates of a particle location and the grid cell containing it. Thus the *c–space* method has the advantage that no search of the particle's new position is required as for algorithms working in p–space and typically spending the majority of CPU time for global and local search algorithms. With respect to the application of high–performance computers, it is highly beneficial that c–space methods do not require such CPU time–killing search algorithms, which are moreover difficult to parallelize and vectorize.

As mentioned above, for four–way coupling the method how particle–particle collisions are handled is a very critical issue. Nevertheless, a deterministic collision model is taken into account instead of a stochastic collision model often used before (see, e.g., Sommerfeld, 2001). Solely binary collisions are considered here. Following the technique of *uncoupling* developed by Bird (1976), the calculation of particle trajectories is split into two stages:

1. particles are moved based on the equation of motion without inter–particle interactions,
2. the occurrence of collisions during the first stage is examined for all particles. If a collision is found, the velocities of the collision pair are replaced by the post–collision ones without changing their position which is also advantageous for parallelization.

The collision handling itself is carried out in two steps:

(I) In the first step likely collision partners are identified. Since for small time steps only collisions between neighboring particles are likely, substantial computational savings are achieved by dividing the computational domain into virtual cells. Choosing the cell size in such a way that the particles per cell are sufficiently low, the cost of checking collisions is reduced from the order $O(N_p^2)$ to $O(N_p)$, which is crucial for large numbers of particles, e.g. $N_p = O(10^7 - 10^8)$, at high mass loadings. Furthermore, to avoid overlapping cells or the necessity to take the 26 surrounding cells into account during the first step, the search and collision detection procedure is carried out a second time with slightly different cell sizes.

(II) The second step solely takes the particles in one virtual cell into account. Following a suggestion of Chen et al. (1998) the algorithm relies on the assumption of constant velocity within a time step, which is reasonable for the small time step sizes applied in LES. Based on the assumption of linear displacements during a time step, it is possible to de-

tect the collision of two particles by purely kinematic conditions, i.e., (i) the two particles have to approach each other and (ii) their minimum separation within a time step has to be less than the sum of their radii. If a collision is detected, the velocities of the colliding particles are changed according to a hard sphere inelastic collision. The measure of inelasticity is generally expressed by a restitution coefficient currently set to unity. At present, friction is not taken into account for the collisions. Thus, solely the velocity components in collision–normal direction are changed by the collision. To achieve this, the Cartesian velocity components are transformed to the collision–normal direction prior to collision and re-transformed after collision.

For the interaction of particles with rigid walls, currently two different boundary conditions can be applied: (i) The particle sticks at the wall and is consequently removed from the computational domain, or alternatively (ii) the particle rebounds fully elastically. This implies that the sign of the velocity component normal to the wall is inverted and all other components are kept.

TEST CASES AND RESULTS
Plane Channel Flow

As a workhorse to validate the entire methodology the turbulent particle–laden plane channel flow was studied in great detail. A variety of cases were considered, including different physical influences (i.e. flow Reynolds numbers, different Stokes numbers of the particles, different mass loadings up to 100%, different particle/fluid density ratios, one–, two– and four–way coupling) and different numerical influences (e.g. grid resolutions, interpolation schemes, SGS fluctuations for the particles).

The results shown here rely on the recently published experiments by Benson et al. (2005). The Reynolds number based on the bulk velocity U_B and the channel half–width δ was Re = 11,900, the ratio of particle diameter to channel half–width was $d_p/\delta = 0.0075$ ($d_p = 150\mu$m), the ratio of particle to fluid density was $\rho_p/\rho_f = 2061$ and the mass loading was $\Phi = 20\%$. The computational domain was $2\pi\delta \times \pi\delta \times 2\delta$ in streamwise, spanwise and wall–normal direction, respectively. The grid employed had $128 \times 128 \times 128$ cells. In streamwise and spanwise direction an equidistant grid was used. In wall–normal direction the first cell center was located at $\Delta y^+ = 0.65$. Periodic boundary conditions were applied at the streamwise and spanwise boundaries and the no–slip condition at the walls.

The instantaneous flow field and the particle velocities are averaged in both homogeneous directions and additionally in time over a dimensionless time interval of about $\Delta T = 980$ in order to reach a statistically steady state. The velocity fluctuations are scaled with the centerline velocity U_c and the mean quantities with the friction velocity u_τ of the unladen flow.

Figure 1(a) shows the mean particle velocity in comparison with the experimental data of Benson et al. (2005). The computed four–way coupled case is in very good agreement with the measurements. It is obvious that considering the particle–particle interactions leads to a flatter mean velocity profile, which indicates an enhanced momentum transfer between the particles. This is underlined by looking at the par-

ticle wall–normal fluctuations (see Fig. 1(b)), where particle–particle collisions lead to an increase of the fluctuations by a factor of about three with respect to the one–way and two–way coupled case. This is astonishing since the mass loading is only $\Phi = 20\%$. Figure 1(d) shows the mean fluid velocity which is almost not affected by the presence of the particles. The wall–normal velocity fluctuations of the fluid depicted in Fig. 1(e) are significantly attenuated by the particles, which is also surprising for this moderate mass loading. The influence is more pronounced for the four–way coupled simulations. Unfortunately, there are no experimental data available for this case. Figure 1(c) shows the particle streamwise velocity fluctuations, which are flatter in the channel center than the corresponding one–way and two–way coupled calculations. This may be explained by the flatter mean particle velocity profile: If a particle moves from a region with a smaller mean velocity to a region with a larger mean velocity, the difference between the instantaneous particle velocity and the mean velocity is the smaller the flatter the mean profile is. This holds of coarse also for the opposite case.

Cold Flow in a Combustion Chamber

In order to test the code using a more challenging case with practical relevance, a cold flow in a model combustion chamber without swirl was considered. The geometry, depicted in Figure 2, was chosen to match the configuration investigated by Boree et al. (2001). They gained detailed particle and fluid data in a configuration typical for combustion devices. This experimental setup is an excellent test case to get insight into the complicated physical mechanisms governing dense multiphase flows.

The particle–laden air flow with a mean velocity $U_{jet} =$ 3.1 m/s enters the chamber through a circular pipe ($R_{pipe} =$ 10 mm) located on the chamber axis (Fig. 2). The Reynolds number based on the pipe radius and the mean inflow velocity is Re = 2006. The particles with a density ratio of ρ_p/ρ_f = 2100 have diameters varying in the range of $d_p = 22$ to $100\mu m$. The mass loading is $\Phi = 22\%$ or 110%. Clean air enters through an annular ring ($R_i/R_{pipe} = 7.5$, $R_a/R_{pipe} =$ 15) with a mean velocity $U_e/U_{jet} = 1.775$. The gravitational acceleration acts in the main flow direction. The inflow conditions are provided by two additional LES predictions using pipe and annular ring flows with periodic boundary conditions and the same cross–sectional grid. For all computed cases with the same mass loading, the same inflow data are used to reduce the considerations solely to the chamber flow. At the outflow a convective boundary condition and the no–slip condition at the walls are prescribed. The chamber with a length of L/$R_{pipe} = 90$ is discretized by an O–type grid consisting of 13 blocks and about 1.3×10^7 cells. To additionally save CPU time, particles hitting the wall or passing the plane normal to $z/R_{pipe} = 45$ were removed from the domain.

In the following the results of three different LES predictions applying one–way, two–way and four-way coupling are discussed and compared with the experimental data of Boree et al. (2001) for the mass loading of $\Phi = 22\%$. For that purpose the instantaneous flow and particle fields were averaged in time over a time interval of about 6 flow–through times of the chamber and additionally in circumferential direction. For the particle phase the size class of $d_p = 50\mu$m was chosen
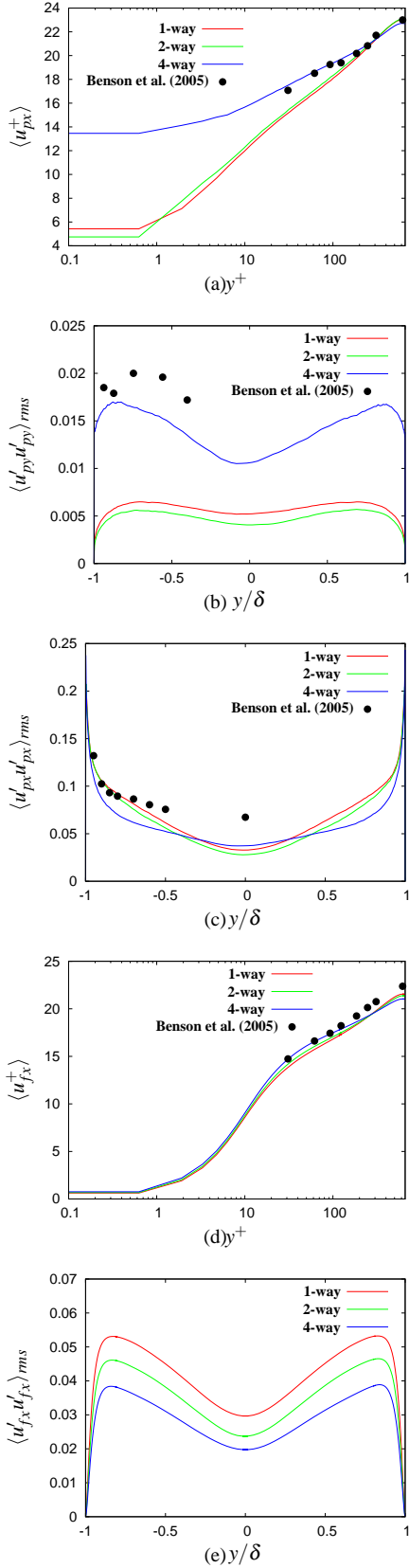
Figure 1. **(a)** Mean streamwise velocity of particles, **(b)** wall–normal velocity fluctuations of particles, **(c)** streamwise velocity fluctuations of particles, **(d)** mean streamwise velocity of fluid, **(e)** wall–normal velocity fluctuations of fluid.
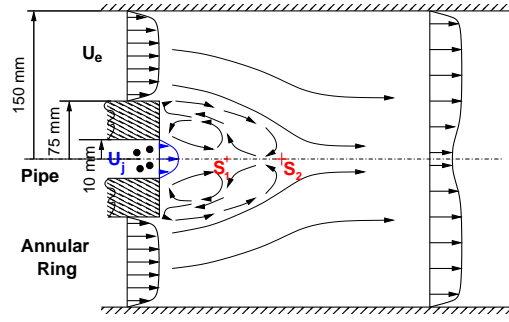
Figure 2. Flow configuration of the combustion chamber.

for the evaluation which is equivalent to the number averaged diameter of the distribution (Boree et al., 2001).

Figure 3(a) depicts the axial velocity along the axis for the flow. As visible, the flow field of the continuous phase is modified by the particulate phase already at this low mass flow rate. The jet developing at the exit of the pipe is stopped rapidly in the recirculating flow forming a first stagnation point S_1 on the axis (see Fig. 2). In the unladen case S_1 is found at about $z/R_{pipe} = 12.5$, whereas for the four–way coupled case the point is shifted downstream to about $z/R_{pipe} = 14.5$. The same trend even more pronounced can be observed in the experimental data. Contrarily, the deviation between the two–way and four–way coupled case is minor, indicating that the role of particle–particle collisions is of less importance for the low mass loading. However, the influence of the particles on the fluid is of major interest. On the other hand the axial velocity of the particles is directly influenced by the fluid flow showing the same trend as visible in Fig. 3(b). A second stagnation point S_2 of the fluid flow is located at the end of the recirculating bubble. Here the differences between the three predicted cases is minor.

Figures 3(c) to 3(h) display velocity profiles at three different axial positions ($z/R_{pipe} = 8$, 16 and 24) for the continuous and the particulate flow. The following observations can be made: 1. Except on the axis, minor deviations are found between the three different simulations at $\Phi = 20\%$. 2. For the measurements differences in the continuous flow for the single and two–phase flow are observed at the outer radii, which are hard to explain. 3. Except for this region, in general a good agreement between predicted and measured data is found.

In Figure 4 the same velocity profiles are depicted for the high mass loading of $\Phi = 110\%$, which still corresponds to a maximum local volume ratio of merely about 0.05 % at the inlet. Solely the cross–section $z/R_{pipe} = 24$ is replaced by $z/R_{pipe} = 20$, since no experimental data are available for the former. Here the deviations between one–way coupling on the one hand and two–way or four–way coupling on the other hand become more pronounced as visible e.g. in Fig. 4(a). Although the predicted curves are presently not very smooth due to insufficient averaging times, the trend is reproduced reasonably. The injected particles induce so much momentum that the stagnation points on the axis disappear and the jet penetrates through the recirculation zone. This also influences the motion of the particles so that no recirculation region is detected on the axis. In contrast to the low mass loading case, here the jet in the center of the combustion chamber outlasts a longer distance and is still visible at $z/R_{pipe} = 20$. As

4
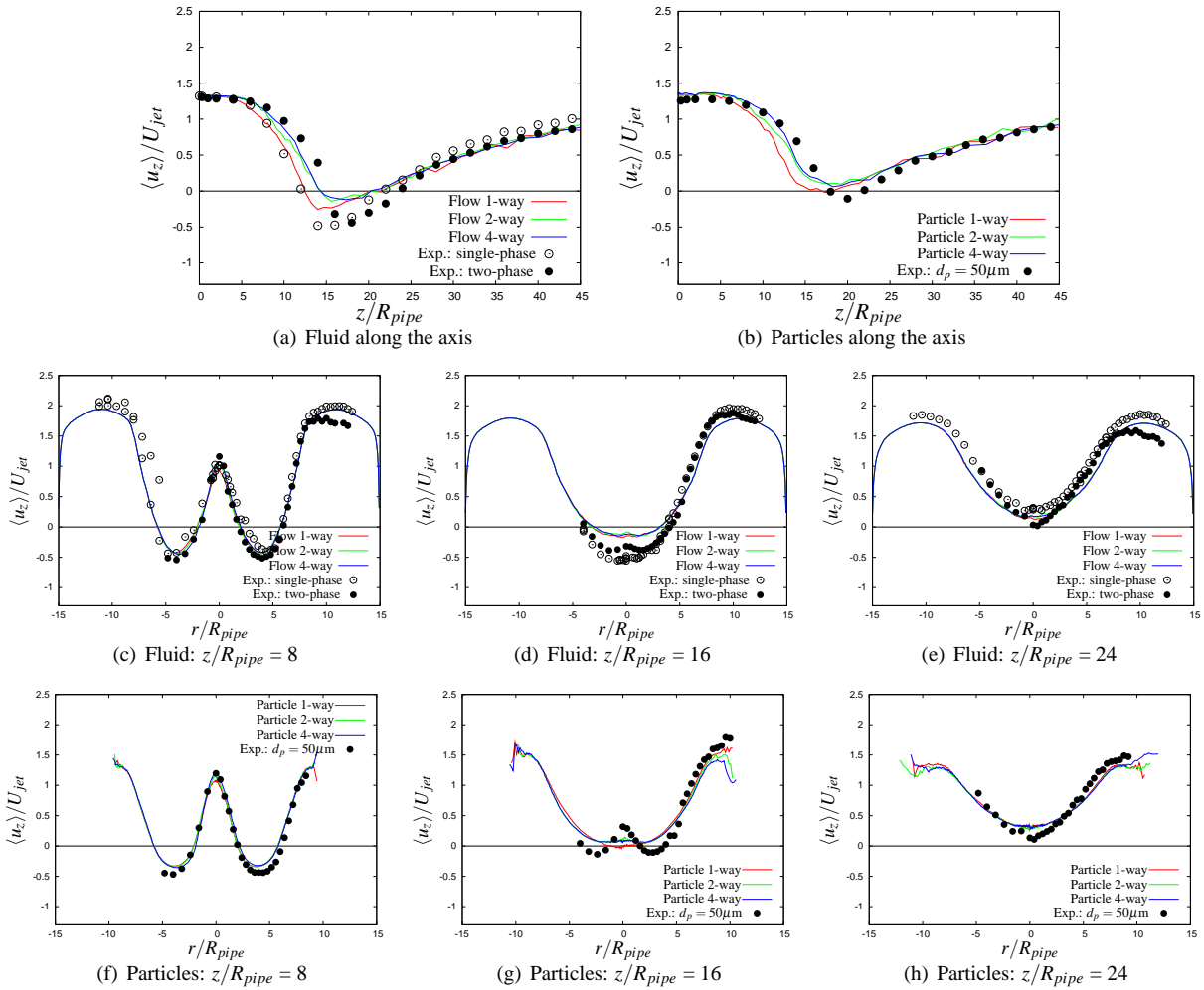
Figure 3. Flow in the combustion chamber at $\Phi = 22\%$: Mean streamwise velocity of fluid and particles ($d_p = 50\mu$m) along the axis and at three different cross–sections; comparison with the experimental data of Boree et al. (2001).

observed before, the particle–fluid interaction is of stronger importance than the inter–particle collisions which coincides with the findings of Boree et al. (2001) emphasizing the impact of particle–fluid correlations. Nevertheless, compared to $\Phi = 22\%$ the influence of particle–particle collisions slightly increases for the higher mass loading. Both the two–way and the four–way coupled simulations deliver reasonable agreement with the experimental data of Boree (2001).

CONCLUSIONS

Simulations with high mass loadings > 100% were carried out with an enhanced Euler–Lagrange algorithm including particle–particle collisions based on a deterministic model and working on curvilinear block–structured grids. Nevertheless, the CPU time required for the collision detection and handling took less than 10% of the total time demonstrating that the code is highly efficient. The methodology was first tested based on the standard channel flow case and then applied to a realistic application. Close agreement is found between the two–way and four–way coupled simulations and the measurements.

REFERENCES

Bardina, J., Ferziger, J.H., Reynolds, W.C., 1980, "Improved Subgrid–Scale Models for Large Eddy Simulations", AIAA Paper, 80–1357.

Benson, M., Tanaka, T., Eaton, J.K., 2005, "Effects of Wall Roughness on Particle Velocities in a Turbulent Channel Flow", Trans. ASME J. Fluids Eng., vol. 150, pp. 250–256.

Bird, G.A., 1976, "Molecular Gas Dynamics", Claredon.

Boree, J., Ishima, T., Flour, I., 2001, "The Effects of Mass Loading and Inter–Particle Collision on the Development of Polydispersed Two-Phase Flow Downstream of a Confined Bluff Body", J. Fluid Mech., vol. 443, pp. 129–165.

Breuer, M., 1998, "Large Eddy Simulation of the Sub–Critical Flow Past a Circular Cylinder: Numerical and Modeling Aspects", Int. J. Num. Methods Fluids, vol. 28, pp. 1281–1302.

Breuer, M., 2002, "Direkte Numerische Simulation und Large–Eddy Simulation turbulenter Strömungen auf Hochleistungsrechnern", Habilitationsschrift, University of Erlangen–Nürnberg, Germany, ISBN: 3–8265–9958–6.

Breuer, M., Baytekin, H.T., Matida, E.A., 2006, "Prediction of Aerosol Deposition in 90° Bends Using LES and an
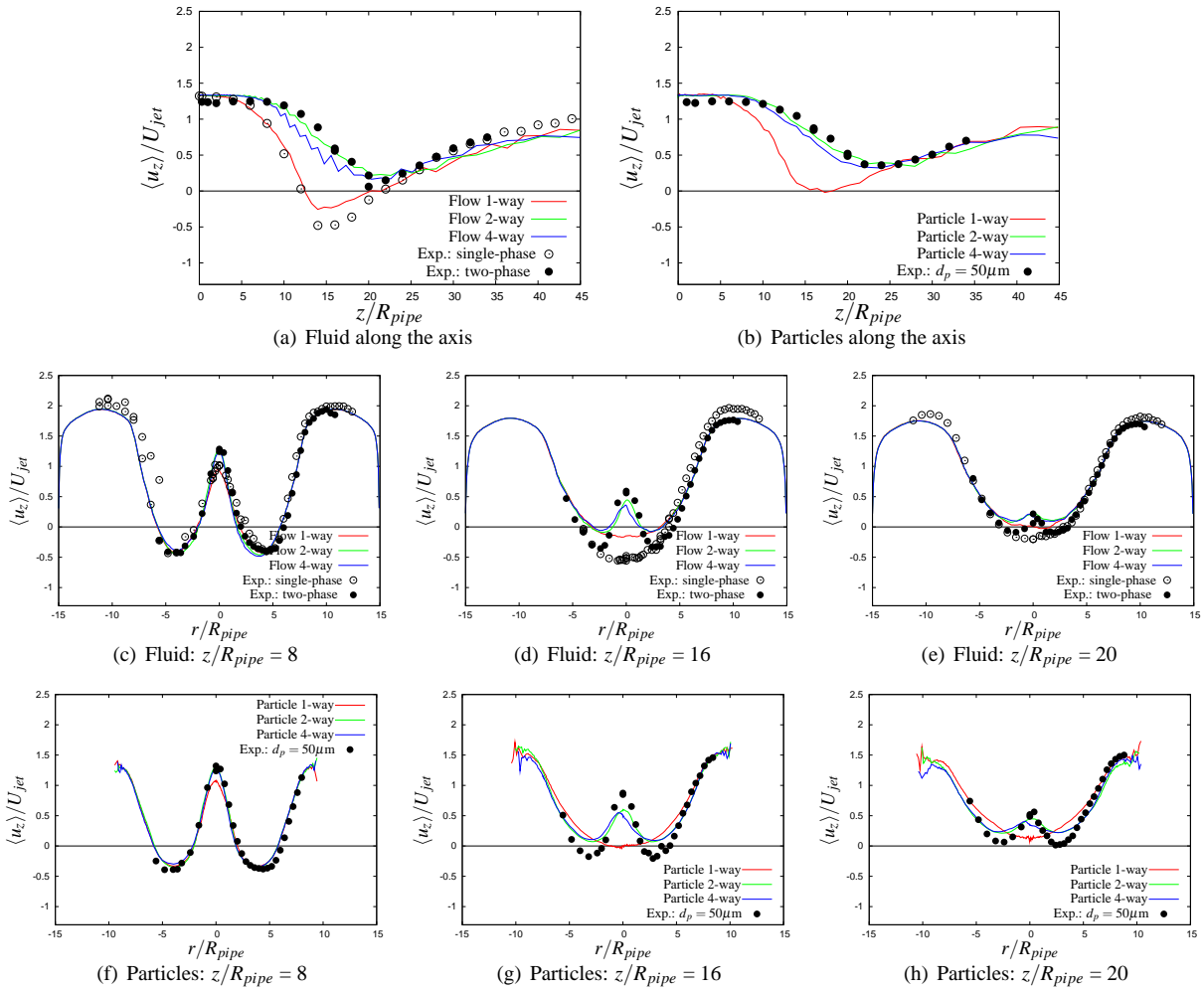
Figure 4.   Flow in the combustion chamber at $\Phi = 110\%$: Mean streamwise velocity of fluid and particles ($d_p = 50\mu$m) along the axis and at three different cross–sections; comparison with the experimental data of Boree et al. (2001).

Efficient Lagrangian Tracking Method", J. Aerosol Science, vol. 37, pp. 1407–1428,

Breuer, M., Matida, E.A., Delgado, A., 2007, "Prediction of Aerosol Drug Deposition Using an Eulerian–Lagrangian Method Based on LES", Int. Conf. on Multiphase Flow, July 9–13, 2007, Leipzig, Germany.

Chen, M., Kontomaris, K., McLaughlin, J.B., 1998, "Direct Numerical Simulation of Droplet Collisions in a Turbulent Channel Flow, Part I: Collision Algorithm", Int. J. Multiphase Flow, vol. 24, pp. 1079–1103.

Crowe, C.T., Sharma, M.P., Stock, D.E., 1977, "The Particle-Source-In-Cell (PSI-CELL) Model for Gas-Droplet Flows", Trans. ASME J. Fluids Eng., vol. 99, pp. 325–322.

Germano, M., Piomelli, U., Moin, P., Cabot, W.H., 1991, "A Dynamic Subgrid–Scale Eddy–Viscosity Model", Phys. Fluids A, vol. 3(7), pp. 1760–1765.

Lilly, D. K., 1992, "A Proposed Modification of the Germano Subgrid–Scale Closure Method", Phys. Fluids A, vol. 4(3), pp. 633–635.

Marchioli, C., Armenio, V., Soldati, A., 2007, "Simple and Accurate Scheme for Fluid Velocity Interpolation for Eulerian–Lagrangian Computation of Dispersed Flow in 3D Curvilinear Grids", Computers & Fluids, vol. 36, pp. 1187–1198.

McLaughlin, J.B., 1991, "Inertial Migration of a Small Sphere in Linear Shear Flows", J. Fluid Mechanics, vol. 224, pp. 261–274.

Pozorski, J., Sourabh, V., (2009), "Filtered Particle Tracking in Isotropic Turbulence and Stochastic Modeling of Subgrid–Scale Dispersion", Int. J. Multiphase Flow, vol. 35, pp. 118–128.

Schiller, L., Naumann, A., 1933, "A Drag Coefficient Correlation", VDI Zeitschrift, vol. 77, pp. 318–320.

Smagorinsky, J., 1963, "General Circulation Experiments with the Primitive Equations, I, The Basic Experiment", Mon. Weather Rev., vol. 91, pp. 99–165.

Sommerfeld, M., 2000, "Theoretical and Experimental Modelling of Particulate Flows", Lecture Series 2000-06, von Karman Institute for Fluid Dynamics.

Sommerfeld, M., 2001, "Validation of a Stochastic Lagrangian Modelling Approach for Inter–Particle Collisions in Homogeneous Isotropic Turbulence", Int. J. Multiphase Flow, vol. 27, pp. 1829–1858.